

Article

Influence of Selected Impregnation Materials on the Tensile Strength for Carbon Textile Reinforced Concrete at Elevated Temperatures

Annette Dahlhoff , Cynthia Morales Cruz and Michael Raupach 

Institute of Building Materials Research (IBAC), RWTH Aachen University, Schinkelstr. 3, 52062 Aachen, Germany

* Correspondence: dahlhoff@ibac.rwth-aachen.de

Abstract: Carbon textile reinforced concrete (CTRC) has been investigated in terms of its elevated temperature and fire behavior in order to evaluate the influence of impregnation materials. Elevated temperature tests have already been carried out for material combinations of CTRC. For the tensile strength and the bond behavior between textile reinforcement and concrete, the impregnation of the textile reinforcement is the influencing factor. Impregnation materials such as epoxy-resin (EP) or styrene butadiene rubber (SBR) showed a deterioration of the elevated temperature behavior compared to unimpregnated materials. The aim of this paper is to close the research gap on the elevated temperature behavior of carbon textile reinforced specimens impregnated with silicic acid ester, epoxy-resin, and epoxy-resin additionally surface-modified with quartz sand. For this purpose, stationary and transient tensile tests at elevated temperatures up to 1000 °C were performed. Furthermore, thermal analysis of the impregnation materials was performed to analyze the tensile tests by correlating the chemical examination with the experimental test results, and the ignitability of the reinforcements was studied using single flame tests. For the investigated reinforcement materials, the failure temperature of the specimens increases with decreasing tensile strength load level for all test specimens. In comparison to the epoxy-resin impregnation material, the silicic acid ester impregnation resulted in higher failure temperatures for comparable load levels. The decomposition of the impregnation materials proved to be a decisive factor due to comparatively evaluated thermal analysis.

Keywords: carbon textile reinforced concrete; elevated temperature behavior; impregnation material; epoxy-resin; silicic acid ester; tensile strength test



Citation: Dahlhoff, A.; Morales Cruz, C.; Raupach, M. Influence of Selected Impregnation Materials on the Tensile Strength for Carbon Textile Reinforced Concrete at Elevated Temperatures. *Buildings* **2022**, *12*, 2177. <https://doi.org/10.3390/buildings12122177>

Academic Editor: Ahmed Senouci

Received: 25 November 2022

Accepted: 5 December 2022

Published: 8 December 2022

Publisher's Note: MDPI stays neutral with regard to jurisdictional claims in published maps and institutional affiliations.



Copyright: © 2022 by the authors. Licensee MDPI, Basel, Switzerland. This article is an open access article distributed under the terms and conditions of the Creative Commons Attribution (CC BY) license (<https://creativecommons.org/licenses/by/4.0/>).

1. Introduction

Currently, carbon textile reinforced concrete (CTRC) as a building material is being investigated in the field of concrete construction to be able to realize resource-efficient construction projects with excellent material characteristics [1–5]. For the tensile strength and bond behavior between textile reinforcement and concrete, the impregnation of the textile reinforcement is the influencing factor [2]. In recent years, research focused on the material behavior of CTRC at service temperatures of various fiber, impregnation, and concrete combinations, e.g., [1,2,6]. In addition to these properties, it is essential to consider also the fire and elevated temperature behavior of the components carbon fiber, impregnation, and concrete, as well as the composite CTRC [1,6,7]. For example, impregnation materials such as epoxy-resin or styrene butadiene rubber showed a deterioration of the elevated temperature behavior compared to unimpregnated materials [1,8,9]. The aim of this study is to close the research gap on the elevated temperature behavior of three innovative and further developed impregnation materials of the individual component of carbon roving, as well as the composite with mortar. One commercially available epoxy-resin impregnated

reinforcement used in the field of new construction, one commercially available epoxy-resin impregnated reinforcement with additional surface modification with quartz sand sanding used for repair, and one impregnated with the silicic acid ester (SAE) developed by Lenting et al. [10] are examined.

For this purpose, the strength and temperature characteristics of the investigated reinforcement materials were compared. Based on the investigations, temperature-dependent tensile strength and the reduction factors for the carbon textile reinforcements with the latest version of epoxy-resin and SAE impregnation will be determined and compared with results from previous studies.

For the design of building components under elevated temperatures, standardized requirements and regulations for building materials and components are used [11–13]. According to DIN EN 13501-1 and DIN EN 13501-2 [12,13], building materials are divided into building material classes and building components in fire resistance classes based on fire tests [13,14]. The assignment of the function of a component to performance criteria, according to DIN EN 13501-2 [13], such as load-bearing capacity (R), integrity (E), and thermal insulation (I), results in different minimum requirements for the building material classes and fire resistance for the individual structures. The design of reinforced concrete structures under fire exposure is based on DIN EN 1992-1-2 [11]. For the design, the strength value is reduced by a reduction coefficient for different building materials and applications, cf. Equation (1) [11]:

$$X_{d,\theta} = k_{\theta} \cdot X_k / \gamma_{M,fi} \quad (1)$$

with:

X_k being the characteristic value of a strength or stiffness property for normal temperature design according to DIN EN 1992-1-2 [11];

k_{θ} being the temperature-dependent reduction factor ($X_{d,\theta}/X_k$) for a strength and deformation property;

$\gamma_{M,fi}$ being the partial safety factor for the relevant mechanical building material property for the fire situation. The value of $\gamma_{M,fi}$ is 1.0 unless the National Annex in a country specifies a different value.

Elevated temperature tests determine the strength characteristics of the materials and, based on these, the reduction factor k_{θ} can be derived [11]. For textile reinforcements, this reduction factor is defined as K_T [1,8,15]:

$$K_T = F_T / F_{20\text{ }^{\circ}\text{C}} \quad (2)$$

with:

K_T being the reduction factor;

F_T being the tensile strength at a specific temperature in N/mm^2 ;

$F_{20\text{ }^{\circ}\text{C}}$ being the tensile strength at a temperature of $20\text{ }^{\circ}\text{C}$ in N/mm^2 .

These elevated temperature tests determine the strength reduction by analyzing stationary and transient temperature tests, cf. Figure 1 [15]. Stationary tests are isothermal tests with constant temperature loading until failure. In transient tests, the specimen is heated to failure at a defined load level. Failure occurs due to the temperature-induced reduction in the strength of the specimen. The transient tests allow the reproduction of the fire exposure of a building component [1,15].

The elevated temperature behavior of fiber materials and CTRC have been studied for different textile reinforcements [1,7,15]. First, tests were carried out on carbon fiber reinforced polymer strip. Bisby et al. [16–19] summarized these tests and indicated as expected a decreasing tendency of strength at increasing temperatures. In addition, the results diverge, which is caused by the different fiber materials, as well as the scattering of the material properties under temperature loading, cf. Figure 2a [1].

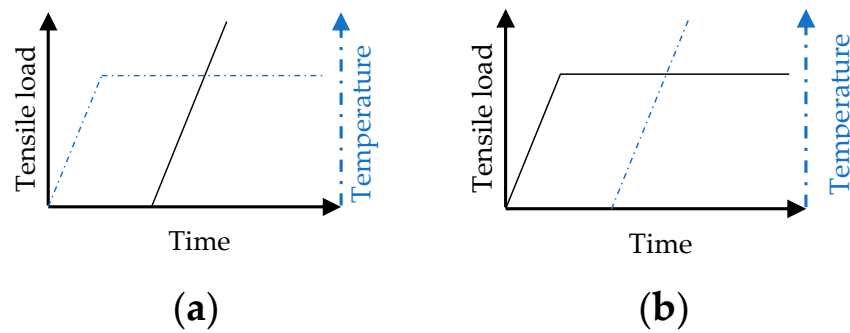


Figure 1. Stationary and transient temperature tests. (a) Stationary; (b) Transient.

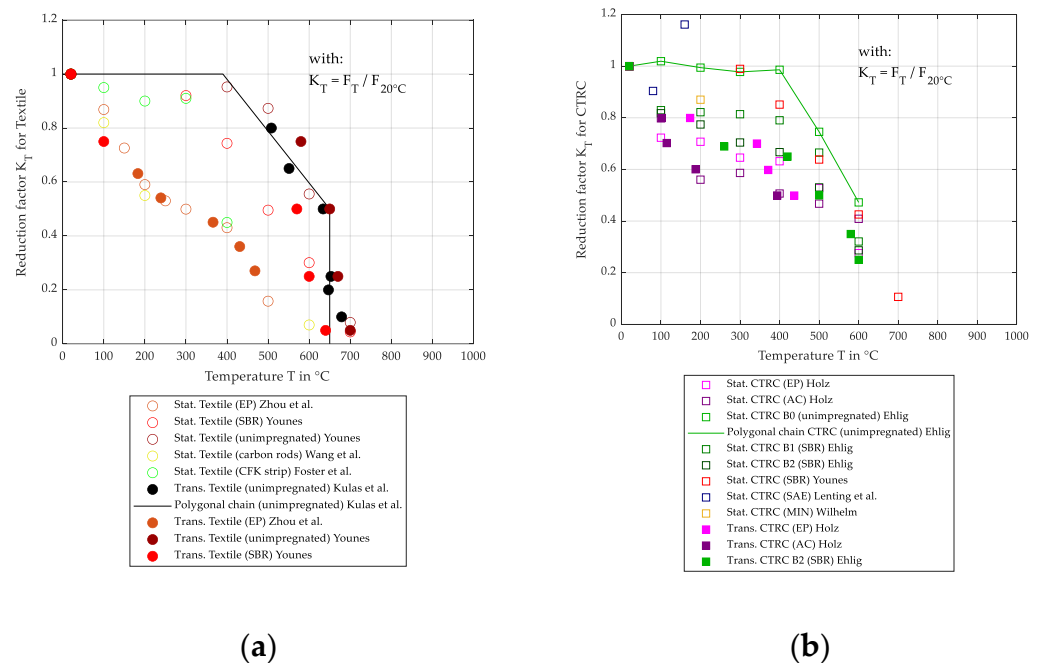


Figure 2. Results from the literature on the elevated temperature behavior for the reduction factor K_T related to the tensile strength at a specific temperature of 20 °C [1,6–10,15,19–21]. (a) Test results of the textile component; (b) Test results of the CTRC.

On carbon bars, stationary investigations up to a temperature of 600 °C with 30 min preheating were carried out in comparison to glass and steel bars by Wang et al. [20], shown in the yellow circles in Figure 2a. The carbon bars showed a strength reduction for higher temperatures greater than the glass bars up to a temperature of 500 °C. Furthermore, the steel bars had the highest load-bearing capacity over the investigated temperature range. On this basis, Zhou et al. [21] performed stationary experiments with 30 min preheating of the material and transient experiments on carbon bars up to 600 °C with a heating rate of 20 °C/min, as shown in the orange circles in Figure 2a. This investigation highlighted the influence of the material's glass transition temperature on strength reduction. In the glass transition temperature range, the strength of the carbon bars showed a significant decrease. In addition, only minor differences between the stationary and transient tests could be detected [21].

Stationary and transient tests were also carried out by Younes [8,22] on styrene-butadiene rubber (SBR) impregnated and unimpregnated carbon fibers (800 tex) with a heating rate of 10 K/min, shown as red and dark red circles in Figure 2a. The SBR impregnation of the fiber strand resulted in a higher rate of strength loss compared to the unimpregnated fiber strand. The unimpregnated fiber strands maintained a constant tensile strength up to a temperature of 500 °C. The test series by Younes [8] indicated an oxidation

reaction of the fiber strands above 500 °C, which resulted in the degradation of the material. Based on the investigations, Younes [8] embedded the materials in concrete with a concrete layer of 1 cm and found a positive effect of the concrete layer on the strength properties for a temperature above 500 °C. As a result, the oxidation process of the carbon could be decelerated by the protective concrete layer [8]. The authors explained that, since the amount of oxygen is many times smaller than in the atmosphere, the oxidation process on carbon filaments embedded in the concrete is much slower. Following the series of tests by Younes [8], unimpregnated carbon fibers (1600 tex) and fine concrete in a high-temperature furnace with a heating rate of 25 K/min were investigated transiently by Kulas et al. [6,15], shown in the black circles in Figure 2a. The trend curve for the carbon fibers showed no reduction in the tensile strength up to a temperature of 395 °C. After exceeding this temperature, the strength decreased until the temperature reached approx. 650 °C. The reduction of tensile strength in the results of Kulas et al. [6] corresponded with the results of Younes [8].

In addition to the described research, Ehlig [9,23] conducted stationary and transient tests on unimpregnated carbon fibers (B0) and two SBR-impregnated carbon fibers with different impregnation ratios, one with an impregnation content of 7.5 wt.-% (B1) and the other of 18 wt.-% (B2), shown in the green colored squares in Figure 2b. With an increasing degree of impregnation, the tensile strength in the range of up to 400 °C decreased to a greater extent. For example, the reduction factor for B2 in comparison to B0 at 600 °C is $\Delta K_T = 0.2$ [9].

Further investigations were carried out by Holz [1] on two textile reinforcement material combinations of CTTC with stationary and transient tests with a heating rate between 6.67 to 9 K/min. The carbon grids were impregnated with epoxy-resin and acrylate, as shown in the purple squares in Figure 2b. Up to a temperature of 200 °C, the tensile strength decreased to a greater extent, and for higher temperatures, thereafter, continuously at a slower rate. In comparison with the thermogravimetric analysis (TGA) of the reinforcement materials, Holz [1] recognized similarities in the individual temperature ranges and soot formation. However, the temperature ranges were different for the material combinations, and thus, not generally applicable to all carbon textile reinforcements [1].

Besides the investigations on polymer impregnation materials, Mechtcherine et al. [24] investigated mineral-based matrices for textile-reinforced concrete, and Wilhelm [7] performed experimental pull-out and tensile strength tests up to 500 °C on mineral-bonded reinforcements (MIN), cf. other squares in Figure 2b. Two special fine cements and a micro silica suspension were used by Wilhelm [7] as an impregnation material for the carbon fibers. The bond behavior for the MIN reinforcement with a water-binder-ratio of 0.8 indicated for pre-tempered specimens at 200 °C a 13% reduction in the tensile strength. Wilhelm [7] concluded this at higher temperatures; however, the mechanical properties were maintained.

In summary, Figure 2 shows the tensile strength results of elevated temperature tests for textile reinforcements with different impregnation materials. The results are presented using the normalized form of the reduction factor K_T calculated according to Equation (2) and the failure temperature representing the corresponding mean value of the test series. Compared to the unimpregnated rovings, the EP impregnation leads to a considerable decrease in the reduction factor for comparable temperatures. Relative to the EP, the SBR impregnation has a lower deterioration of the reduction factor and shows similar behavior to the unimpregnated rovings. For the CTTC, a comparable behavior to the rovings for the EP and SBR impregnation can be observed.

2. Materials

In this study, two commercial carbon textile reinforcements, as well as carbon rovings impregnated with silicic acid ester according to [10], were examined. One carbon textile impregnated with epoxy-resin for new constructions, referred to as CTR-EP, with a rectangular roving axis distance of 21 mm and an equal roving cross-section of 0.91 mm²

in the wrap and weft direction was used, while the second carbon textile for repair was additionally surface modified. In the following, this is referred to as CTR-EP-Sand. The surface modification comprises a subsequent coating of epoxy-resin and quartz sand. In addition to the epoxy-resin impregnated reinforcement, carbon rovings impregnated with silicic acid ester, referred to as CTR-SAE, have a roving cross-section of 1.92 mm^2 [10]. The three investigated materials are shown in the following Figure 3, and the material parameters of the reinforcements are summarized in Table 1.

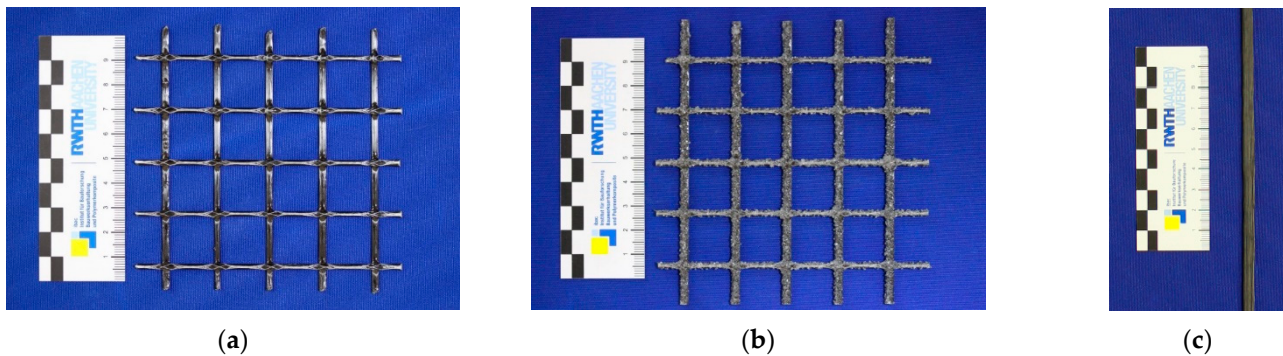


Figure 3. Investigated carbon textile reinforcements. (a) CTR-EP; (b) CTR-EP-Sand; (c) CTR-SAE.

Table 1. Material parameters of the carbon textile reinforcements according to the manufacturer's specification [25].

Reinforcement	Roving Axis Distance	Roving Cross-Section	Textile Cross-Section	Titer	Average Tensile Strength (Wrap Direction)
[—]	[mm]	[mm^2]	[mm^2/m]	[tex]	[MPa]
CTR-EP	21/21	0.90/0.90	43/43	1600	4200 ± 180 ⁽¹⁾
CTR-EP-Sand	21/21	0.90/0.90	43/43	1600	4200 ± 215 ⁽¹⁾
CTR-SAE	-	1.92	-	3450	1550

⁽¹⁾ Measurements performed at the Institute of Building Materials Research (ibac), RWTH Aachen University.

The glass transition temperature T_g was determined using differential scanning calorimetry (DSC). The tests were carried out according to [26,27] under an air atmosphere from 0 to 200 °C at a speed of 10 K/min. The T_g was determined from the point of intersection of the angle bisector (midpoint) during the 2nd heating measurement curve [2]. For the CTR-EP, the T_g based on the DSC measurements at ibac is 101 °C, whereas the T_g for CTR-SAE results in 76 °C. For CTR-EP-Sand, the T_g is not detectable due to the quartz sand residues. TGA was performed for evaluating the decomposition and oxidation process of the impregnation materials CTR-EP and CTR-EP-Sand, according to [28]. To create comparable conditions with the high-temperature furnace, the tests were carried out under atmospheric conditions with oxygen. For CTR-EP the start of pyrolysis was determined at a temperature of 250 °C, cf. Figure 4a. In the range between 250 and 380 °C, a mass loss of 50% for CTR-EP and 20% for CTR-EP-Sand was measured.

For the investigations of the composite, a repair mortar RM-A4, according to [29,30], is used. Based on the investigated carbon textile reinforcements used in the field of repair, the repair mortar RM-A4 was applied [31]. The repair mortar is a polymer-modified cement-based mortar designed for repairing and retrofitting horizontal, vertical, and overhead concrete surfaces with a maximum grain size of 2 mm. The material properties of the mortar are shown in Table 2. The elevated temperature behavior of the RM-A4 is characterized in Figure 5.

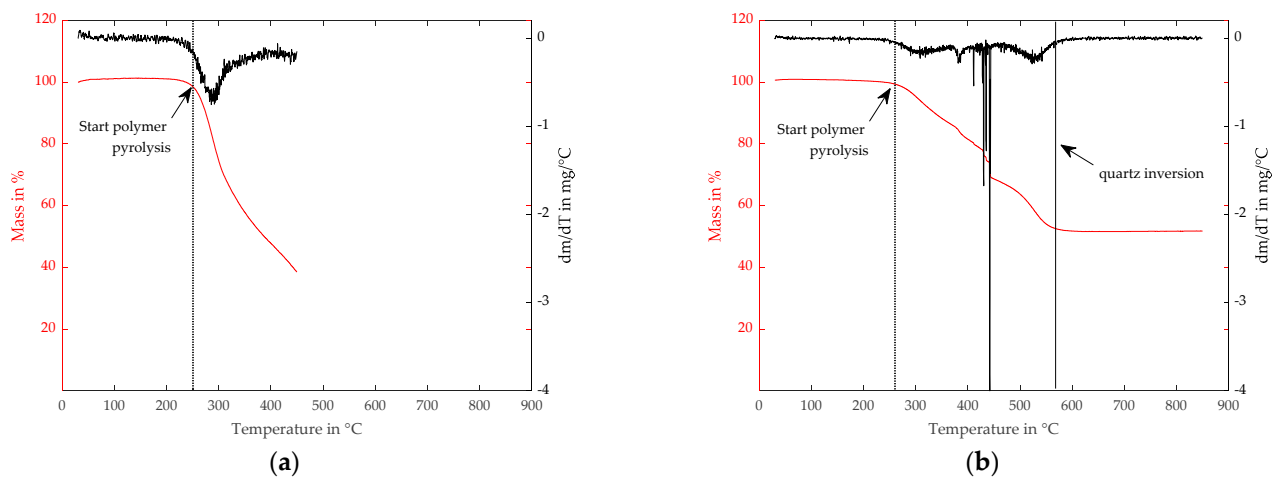


Figure 4. Thermogravimetric analysis. (a) Impregnation material of the CTR-EP; (b) Coating material of the CTR-EP-Sand.

Table 2. Material parameters of the repair mortar RM-A4.

Mortar	Compressive Strength ⁽¹⁾	Bending Strength ⁽¹⁾	Young's Modulus ⁽²⁾
[–]	[MPa]	[MPa]	[GPa]
RM-A4	75 ± 4	11 ± 1.5	24.2 ± 0.1

⁽¹⁾ Measurements performed at the Institute of Building Materials Research, RWTH Aachen University.

⁽²⁾ According to [2].

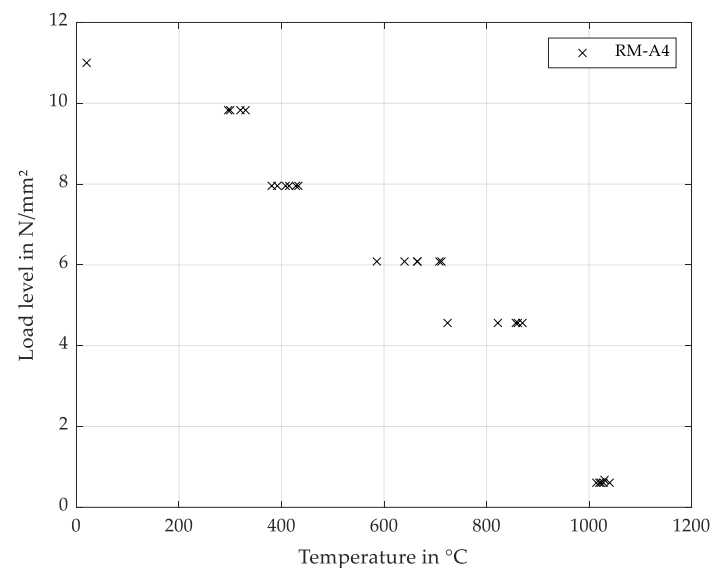


Figure 5. Elevated temperature behavior of RM-A4.

3. Experimental Methods

3.1. Methods

To investigate the elevated temperature behavior of the presented reinforcement materials, transient axial tensile strength tests were conducted. Additional stationary tests were performed at specific temperature ranges at $T = 60/80/100$ °C. In addition to the mentioned investigations, flame tests on the reinforcements were conducted to analyze the differences in flammability [32,33].

Moreover, transient tests were carried out on the CTRC using cylindrical tensile specimens (CTS) consisting of a carbon roving partly prepared out of the presented carbon

textile reinforcements and a mortar layer. Scanning electron microscopy (SEM) images of selected composite specimens were taken and examined after transient tensile testing to visualize the interfaces at different temperature levels.

Table 3 gives an overview of the experimental test series.

Table 3. Overview of the experimental test series.

Experimental Tests	CTR-EP		CTR-EP-Sand		CTR-SAE		
	Testing Load Level ⁽¹⁾	Number of Tests Specimens ⁽²⁾	Testing Load Level ⁽¹⁾	Number of Tests Specimens ⁽²⁾	Testing Load Level ⁽¹⁾	Number of Tests Specimens ⁽²⁾	
	[%]	[–]	[%]	[–]	[%]	[–]	
Transient	100/80/64/50/ 35/30/18/14	10	100/80/64/50/ 35/30/18/14	10	100/50	6	
Roving	Stationary at 60/80 °C and 100 °C	- 5	-	5	-	-	
	Vertical flame test	-	5	-	5	5	
Textile	Single flame test	-	6	-	6	-	
CTRC	Transient	100/80/64/50/ 35/30/18/14	10	100/80/64/50/ 35/30/18/14	10	100/75/50	4
	SEM	100/64/50/14	1	100/64/50/14	1	-	-

⁽¹⁾ Testing load level based on experiments at a room temperature of 20 °C (100%). ⁽²⁾ Number of test specimens per testing load level.

3.2. Experimental Setup and Testing Procedure

The elevated temperature tests were carried out in a high-temperature furnace capable of reaching temperatures up to 1100 °C. In combination with a 100 kN universal testing machine, the high-temperature furnace enables stationary and transient tests with a heated specimen length of 40 cm, cf. Figure 6a. The installed specimens are cooled with a cooling device in the clamping. All tests were carried out at a test speed of 2 mm/min. For the stationary tests, the specimens were heated before testing for 15 min. Preliminary tests indicated the furnace settings to accurately reproduce the uniform temperature curve, according to [11]. For the high-temperature furnace used, a presetting of 100 °C/min provided equivalent results, cf. Figure 7a. In addition, temperature sensors were installed inside the CTRC on the middle specimen height at the roving, and the temperature difference between the high-temperature furnace and the temperature sensors inside the CTS during the heating process was measured, cf. Figure 7b.

For the test series, the component of the carbon textile reinforcement was investigated on rovings. For this purpose, 80 cm long rovings were extracted in the wrap direction from the textile carbon reinforcement, whereas the CTR-SAE rovings were cut to the corresponding length. The roving ends were glued with a cold-curing sand-filled epoxy-resin in the anchorage. The anchorage, 100 mm on each side, consisted of a steel hull with an outer diameter of 24 mm at the top and a screw with an inner thread and diameter of 12 mm at the bottom for the attachment to the cooling system inside the furnace, as shown in Figure 8a.

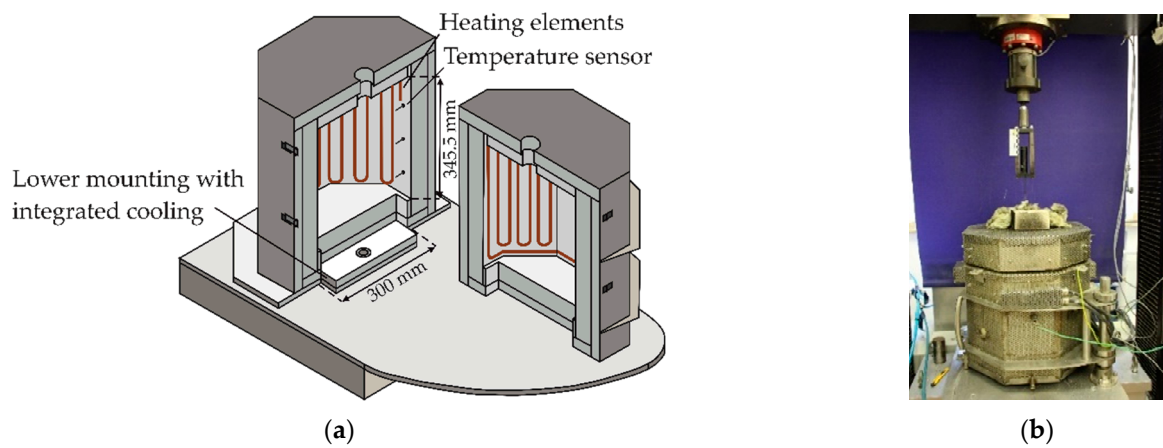


Figure 6. High-temperature furnace. (a) Schematic drawing adapted from the image source (IWM and IPAK, RWTH Aachen University); (b) Test setup in the laboratory.

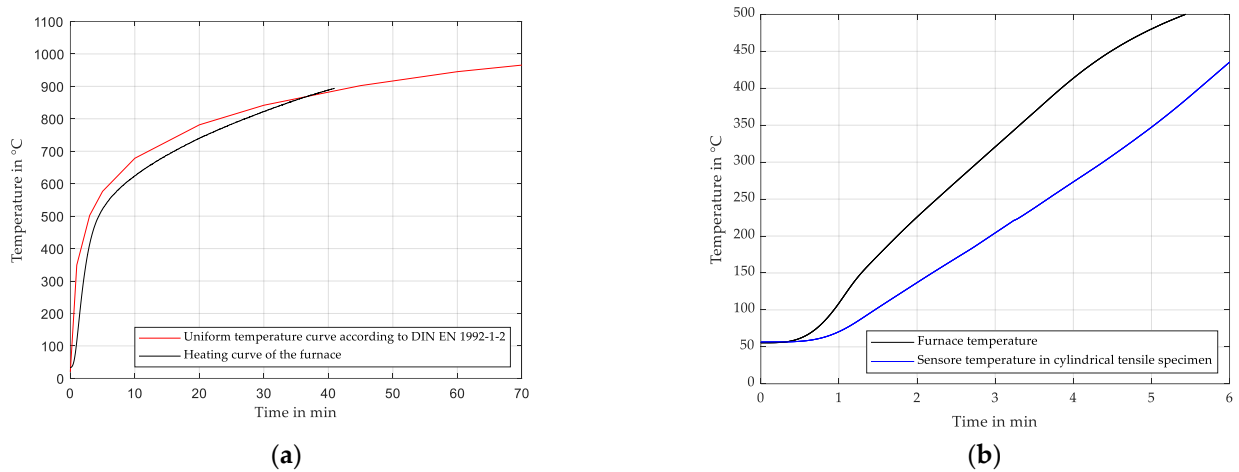


Figure 7. Temperature over time curves. (a) Comparison of the uniform temperature curve with the setup on the high-temperature furnace adapted from [11]; (b) Comparison of the temperature in the high-temperature furnace and inside the CTS.

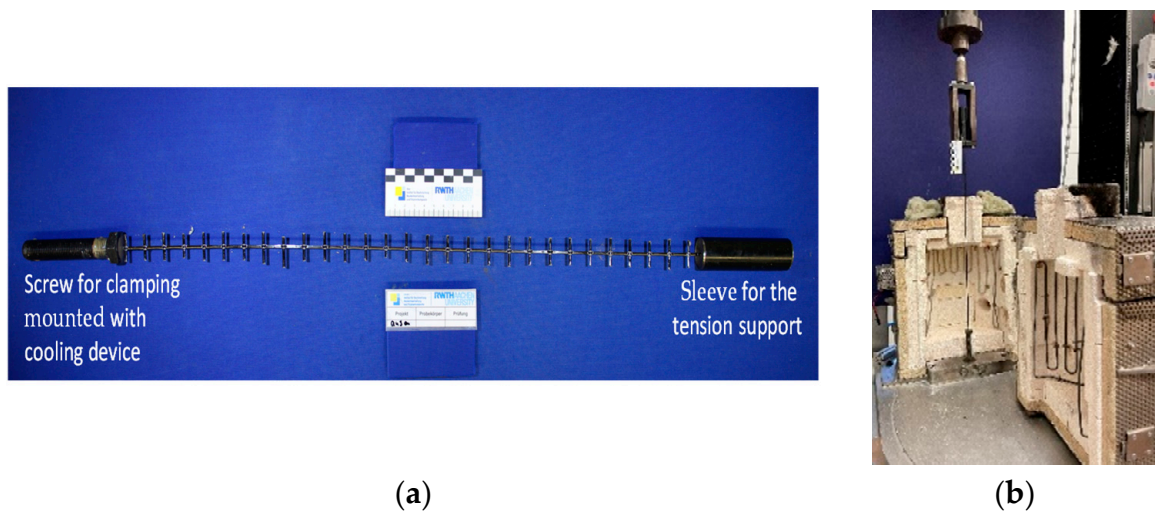


Figure 8. Test setup for the investigation of the roving component. (a) Exemplary photograph of the roving specimen CTR-EP; (b) Stationary and transient test setup in the high-temperature furnace for CTR.

Additionally, two flame test series were carried out on the reinforcement materials in a flammability tester. On the one hand, the vertical single flame source test, according to UV 94 [32], for the ignition and after-flaming behavior was carried out, referred to as VFT. For this, 125 mm long wrap rovings cut from the reinforcement grid were used. The rovings were installed in support and cotton wool was placed underneath in a tray, cf. Figure 9a. Before and after each test, the roving and cotton wool were weighed. The samples were flamed for 10 s with a burner at a 45° angle. The flame was then withdrawn at least 150 mm from the specimen, while the after-flaming time was measured. Once the flame was extinguished, the burner was again placed under test specimen for additional 10 s and the after-flaming time was measured. In addition, the highest flame height was measured at the lower sample edge in this test series.

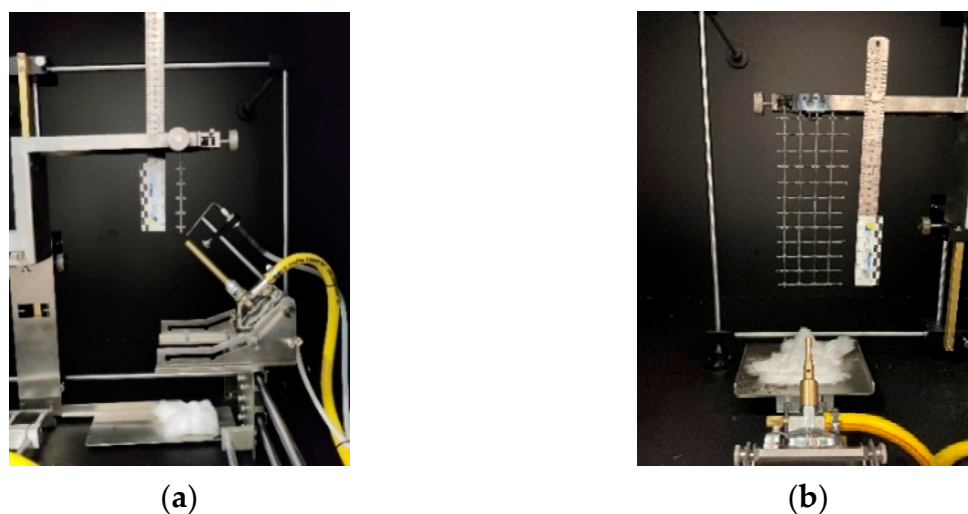


Figure 9. Vertical flame test setup in the burning chamber, according to [32,33]. (a) VFT on single roving; (b) SFT on textile reinforcement.

To further investigate the ignitability and classification of the epoxy-resins tests according to DIN EN ISO 11925-2 [33] were carried out, referred to as SFT. Textile reinforcement specimens in wrap direction, measuring 250×90 mm, were prepared and placed in the mounting, cf. Figure 9b. Here, as well, the weight of the specimen and cotton wool was measured before and after the ignitability test. The burner was ignited and the flame height was set to 20 mm. The specimen was spot-flamed for 15 s at the middle bottom edge. The after-flaming time and the maximum flame height of 150 mm above the flame point were determined.

For the test series of the CTRC, cylindrical tensile specimens (CTS) were produced, cf. Figure 10a. For this purpose, a roving made from the reinforcement grid in the wrap direction was cast in a sleeve and a screw, as described before. Around the 80 cm long roving, a 50 cm long cylindrical mortar casing with a 1 cm concrete cover was produced. A concrete cover of 1 cm is often used for the rehabilitation of concrete structures composed of CTRC [2]. The mortar was mixed according to the manufacturer's specifications in a ratio of solid to water weight content of 1:0.13, applied to the formwork and compacted with vibrations. The CTS were stored in a humid climate for 7 days and stripped of the formwork after these 7 days. Afterwards, the specimens were stored in a climate room at a temperature of 20 ± 1 °C and relative humidity of $53 \pm 8\%$ until the age of 28 days. Subsequently, the specimens were weighed and stored in an aerated heating cabinet at a temperature of 60 °C until the constant mass of the solid content was reached. From the investigated CTS, one sample for each of the four selected load levels was prepared and examined using scanning electron microscopy (SEM). The results of the temperature influence on the composite were investigated using SEM with secondary electron analysis, backscattered electron analysis, and energy dispersive X-ray spectroscopy.

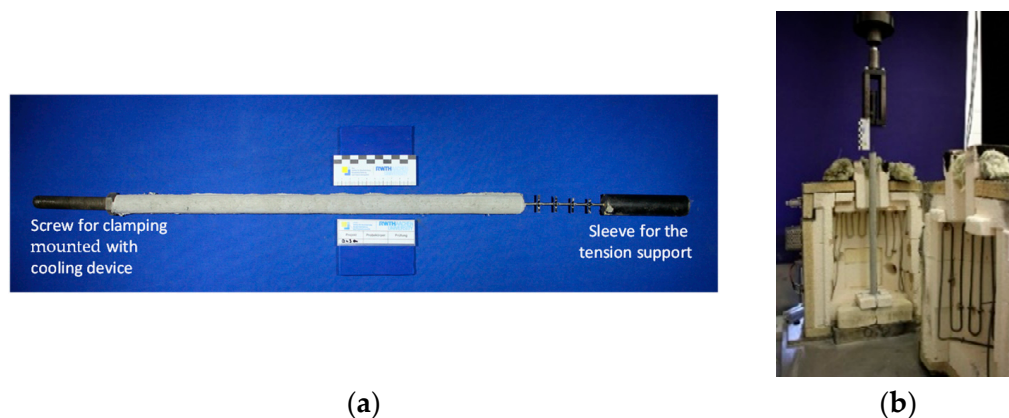


Figure 10. Test setup for the investigation of the CTS. (a) Exemplary photograph of the CTS for CTR-EP; (b) Test setup in the high-temperature furnace for CTS.

4. Results

4.1. Experimental Results of the CTR

4.1.1. Transient Test Results

First, tensile strength tests were conducted at a room temperature of 20 °C as reference. The epoxy-resin impregnated carbon rovings CTR-EP and CTR-EP-Sand achieved on average nearly three times higher tensile strength values compared to CTR-SAE, cf. Figure 9a. The unimpregnated fiber tensile strength specified by the manufacturers was $>4000 \text{ N/mm}^2$ for CTR-EP/CTR-EP-Sand and 4400 N/mm^2 for CTR-SAE at room temperature [10,25]. For the CTR-EP/CTR-EP-Sand, a utilization rate of the tensile strength of 95% can be assumed, whereas the CTR-SAE utilization rate was 35%.

As expected, the results of the transient roving tensile tests showed an increase in failure temperature with decreasing load levels. Compared to the unimpregnated fibers, the CTR-EP and CTR-EP-Sand showed a decrease of up to 70% in the failure temperature for comparable load levels. The CTR-SAE approximates the unimpregnated fiber curve by Kulas et al. [6]. Furthermore, it can be observed that at load levels $K_T \geq 0.35$ the failure temperature of CTR-EP-Sand is higher up to a temperature difference of 50 °C compared to CTR-EP. This effect could be related to the higher polymer content of the surface-modified carbon textiles used in the subsequent coating. The authors assume that the polymer coating acts like a heat shield and therefore leads to a higher failure temperature. Further analysis of these results will follow in Section 4.1.3. For the CTR-EP test series, the largest standard deviations can be seen at the load levels $K_T = 0.35$ and $K_T = 0.65$. This is probably attributed to the glass transition temperature of 101 °C, and the onset of the degradation of the impregnation material. The start of the thermal decomposition as pyrolysis was determined at a temperature of 235 °C, cf. Figure 11a.

Depending on the way of evaluation, different interpretations of the results are possible. If different impregnation materials are compared with each other, an evaluation comparing the reduction factor K_T should be considered with caution. In order to investigate the influence of the temperature of a reinforcement and to determine design criteria, the representation in terms of K_T is advisable. For a reduction factor of $K_T = 0.5$, the failure temperature of SAE-impregnated roving is measurably higher than that of epoxy-resin-impregnated rovings. The difference in failure temperature between CTR-EP and CTR-SAE at a reduction factor of $K_T = 0.5$ is 384 °C. However, comparing the absolute load levels at 770 N/mm^2 , the average failure temperature of the CTR-SAE rovings is merely 50 °C higher, cf. Figure 11a. Thus, for CTR-SAE in the loading at $K_T = 0.5$, an increased temperature resistance is shown, while for the absolute tensile strengths no improvement is evident. Therefore, when investigating the elevated temperature behavior of textile reinforcements, the absolute tensile strengths should also be recorded and considered. Furthermore, the test series showed that the failure temperatures do not exceed 600 °C even at lower load

levels. This is attributed to the decomposition of the carbon fiber occurring at 600 °C under an oxygen supply [34].

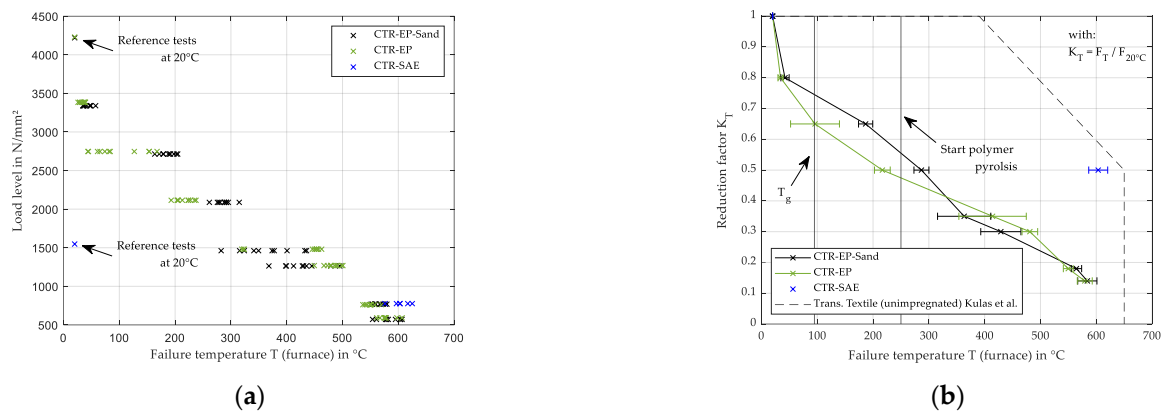


Figure 11. Roving tensile transient test. (a) Failure temperature measured in the furnace due to varying load levels (individual values); (b) Failure temperature as mean value with standard deviation for the reduction factor K_T [6].

Given the data basis, the results were fitted into polygonal chains for the epoxy-resin-impregnated rovings. The CTR-EP and CTR-EP-Sand indicated increasing strength reduction between $K_T = 0.8$ – 1.0 , which rather suggests a bilinear curve fit. To further investigate these results, stationary tests were performed at temperature levels of 60/80/100 °C, respectively, cf. Section 4.1.2.

During the transient elevated temperature tests of the roving CTR-EP and CTR-EP-Sand, smoke development and flame formation were detected. Videos during the tests in the high-temperature furnace indicated flame formation starting at 240 °C. This flame formation can influence the results of the tests, especially the decomposition of the impregnation. The flame formation can be attributed to pyrolysis of the polymer as a result of the elevated temperatures. Together with oxygen, these gaseous short-chain pyrolysis gases form a self-igniting mixture [35]. To investigate the influence of this phenomenon, the textile reinforcement materials were subjected to flame testing.

4.1.2. Stationary Test Results

The stationary tests indicated reduced tensile strength for the increasing test temperature. Based on the normally distributed results, verified with parametric testing, according to Kolmogorov–Smirnov and Shapiro–Wilk, as given, for example, in [36], the Grubbs statistical outlier test was performed [37]. The outliers can be explained by possible pre-damage from the factory or during sample preparation and were neglected in the further course of the analysis.

The individual tensile strength values indicate reduction factors between $K_T = 0.7$ – 1.0 , cf. Figure 12a. On average, the roving tensile strength at a test temperature of 60 to 80 °C decreased by only 5 to 15%, compared to the test at 20 °C. Compared to the transient tests, the tensile strength at test temperature of 60 to 80 °C shows higher values, which exceed the regression line, cf. Section 4.1.1. This can be related to the high utilization of the rovings and the corresponding pre-damage of the impregnation material, cf. Section 4.1.1.

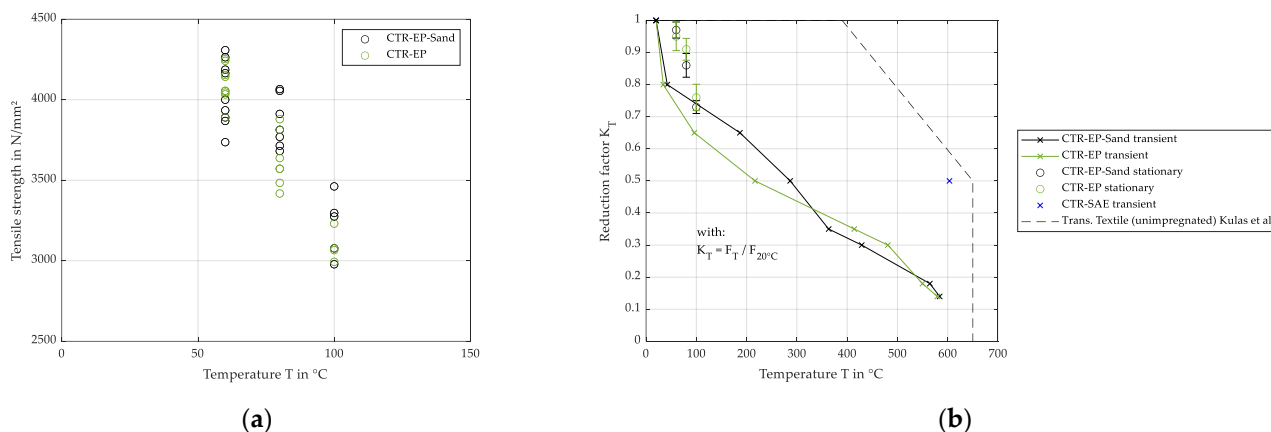


Figure 12. Roving tensile test. (a) Stationary test temperature due to varying load levels (individual values); (b) Transient and stationary test temperatures as mean value with standard deviation for the reduction factor K_T [6].

For the tests at 100 °C, the reduction factor $K_T = 0.7$ corresponds to the transient test results, cf. Figure 12b. The results of the test series indicated consistent tensile strengths in comparison with epoxy-resin impregnated roving materials known from the literature [21].

4.1.3. Flame Test Results

For further scientific investigation, the reinforcement materials were flamed in a burning chamber to examine the influence of the additional polymer coating in terms of flammability, combustibility, and smoke development.

On the one hand, the VFT according to [32] was carried out, cf. Figure 13. It was found that the CTR-SAE reinforcement showed no after-flaming and had an average weight loss of only 4%, cf. Table 4. In comparison, CTR-EP exhibited an after-flaming behavior, and in some tests, the cotton wool was ignited due to formed drops. In the case of the burned CTR-EP, a weight loss of 46% was recorded. Compared to the CTR-EP, the CTR-EP-Sand had a higher after-flaming time with a mean value of 70.6 s and a high number of falling drops $n = 26.4$. This can be attributed to the additional surface modification. Droplets of the molten polymer formed around the quartz sand and dripped onto the wool due to their higher weight. Furthermore, the surface modification lead to an increase in the after-flaming time of 39.28 s.

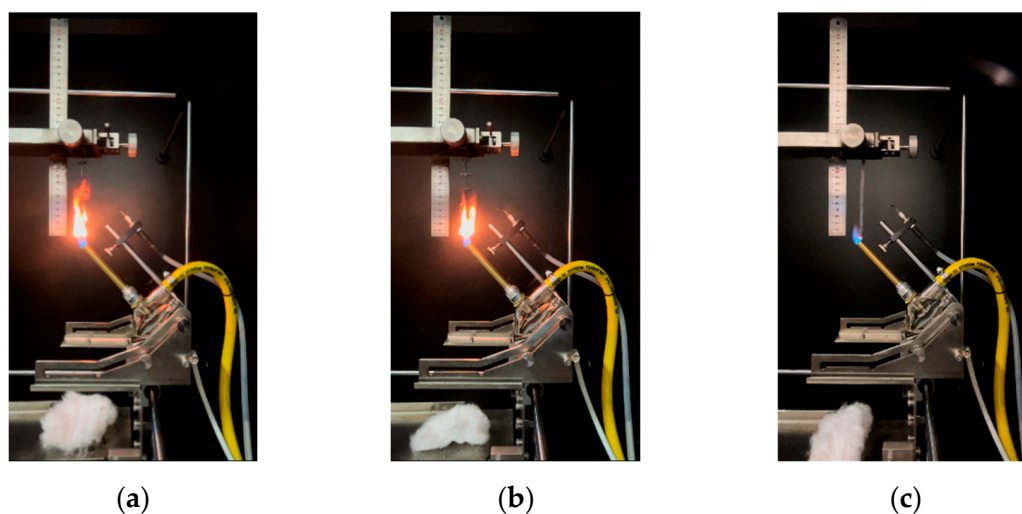


Figure 13. VFT tests after 5 s flaming time. (a) CTR-EP; (b) CTR-EP-Sand; (c) CTR-SAE.

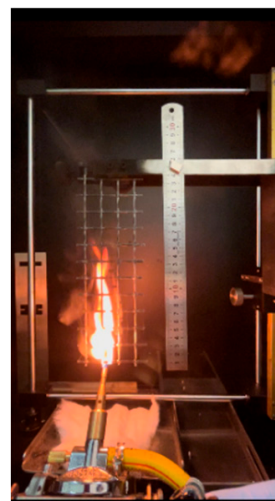
Table 4. Flame Test Results, according to VFT. Mean values of the test series.

Reinforcement	Weight Roving		After Flaming Time	Number of Drops	Maximum Flame Height ⁽¹⁾
	Before Testing	After Testing			
[–]	[g]	[g]	[s]	[–]	[cm]
CTR-EP	0.70	0.32	31.32	1.0	14.0
CTR-EP-Sand	1.87	0.61	70.60	26.4	12.1
CTR-SAE	0.79	0.76	0	0	0

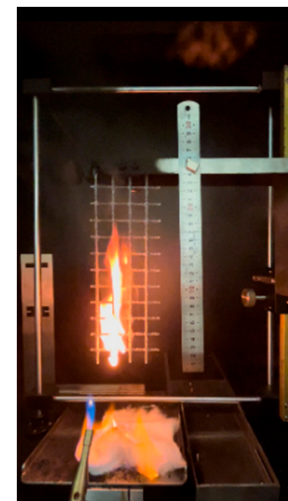
⁽¹⁾ Measured from the lower sample edge.

Accordingly, the SAE-impregnated rovings are not flammable, while flame formation occurs for the epoxy-impregnated rovings.

The flammability of the materials under direct flame exposure was also studied using the SFT, according to [33], cf. Figure 14. For this purpose, the fire behavior, as well as the smoke development of epoxy-resin impregnated reinforcements were investigated. Moreover, in this series of experiments, the total duration of the flame process was longer for CTR-EP-Sand compared to CTR-EP by approximately 44 s. The falling of single droplets and the ignition of the cotton wool was also observed as previously described for CTR-EP-Sand, resulting in a weight reduction of both the roving and cotton, cf. Table 5. In addition, smoke emission was detected in both materials. For the epoxy-impregnated textile reinforcement material, it can be seen after the test that the only part of the test specimen burns off. The flames did not spread to the entire specimen.



(a)



(b)

Figure 14. SFT in the burning chamber. (a) CTR-EP; (b) CTR-EP-Sand.**Table 5.** Flame test results, according to SFT. Mean values of the test series.

Reinforcement	Weight Roving		Weight Cotton		Total Duration of Test	Flame Height 150 mm ⁽¹⁾	Highest Flame Height	Smoke Emission
	Before Test	After Test	Before Test	After Test				
[–]	[g]	[g]	[g]	[g]	[s]	[s]	[mm]	[–]
CTR-EP	6.74	4.81	5.26	4.09	94	14	308	✓
CTR-EP-Sand	17.46	13.18	5.10	2.81	138	21	275	✓

⁽¹⁾ Measured from the lower sample edge.

The single fire tests confirm the flame and smoke development observed in the transient roving tensile tests. It can be determined that the CTR-EP-Sand reinforcement in both test variants developed flames slowly and were ignitable with more material falling off in separate droplets than the CTR-EP reinforcement. The higher after-flaming time could be attributed to the higher polymer content and could explain the higher failure temperature values of CTR-EP-Sand in the elevated temperature tests, cf. Figure 11b. The prevailing flame formation in the furnace during transient tensile testing of the rovings was consistent with the results of the single flame test.

4.2. Experimental Results of the CTRC

Transient Test Results

In the transient laboratory tests on CTRC using cylindrical tensile specimens (CTS), an increase in the failure temperature for decreasing load levels was found, analogous to Section 4.1.1. Already during loading, it was observed, as shown in [2], that more and smaller cracks formed in the CTSs for the surface-modified CTS-EP-Sand than with the CTS-EP reinforcement, cf. Figure 15.

However, compared to CTS-EP, there was no measurable difference on the failure temperature for CTS-EP-Sand. Furthermore, the CTS-SAE specimens failed at a significantly higher temperature for comparable reduction factors. Compared with CTS-EP and CTS-EP-Sand, the increase in failure temperature of the CTS-SAE was lower at the investigated load levels. Thus, a high failure temperature can already be achieved at $K_T = 0.75$, which can be attributed to the impregnation decomposition.

In the experimental test results, two sections can be obtained, cf. Figure 16b. For the first section ($K_T > 0.64$), the increase in failure temperature correlated to the reduction factor is higher. However, the increase of failure temperature for $K_T < 0.64$ is lower. This can be related to the decomposition of the impregnation, as described in Section 2. After the complete decomposition of the impregnation, the failure is related to the oxidation of the fiber. Due to the protective mortar layer the failure temperature can be increased up to 800 °C. In addition, at increased load levels, the utilization of the fiber is elevated. The carbon fibers are strained to a greater extent. Due to this strain, pre-damage can occur and the decomposition process of the carbon fiber can proceed faster.

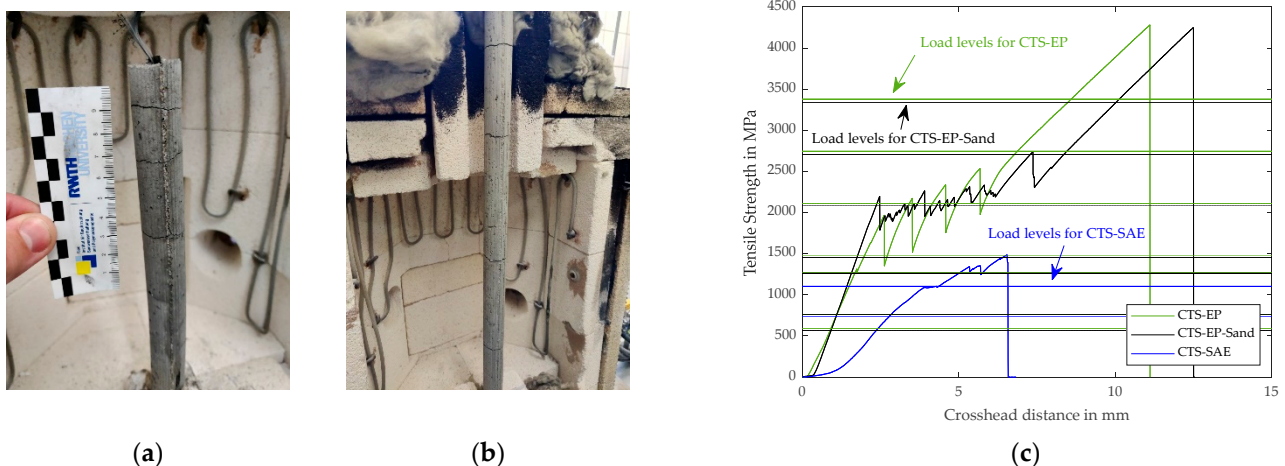


Figure 15. Crack formation in the CTS after tensile tests at 20 °C. (a) CTS-EP-Sand; (b) CTS-EP; (c) Representative tensile strength-deformation curves of the reference test at room temperature 20 °C.

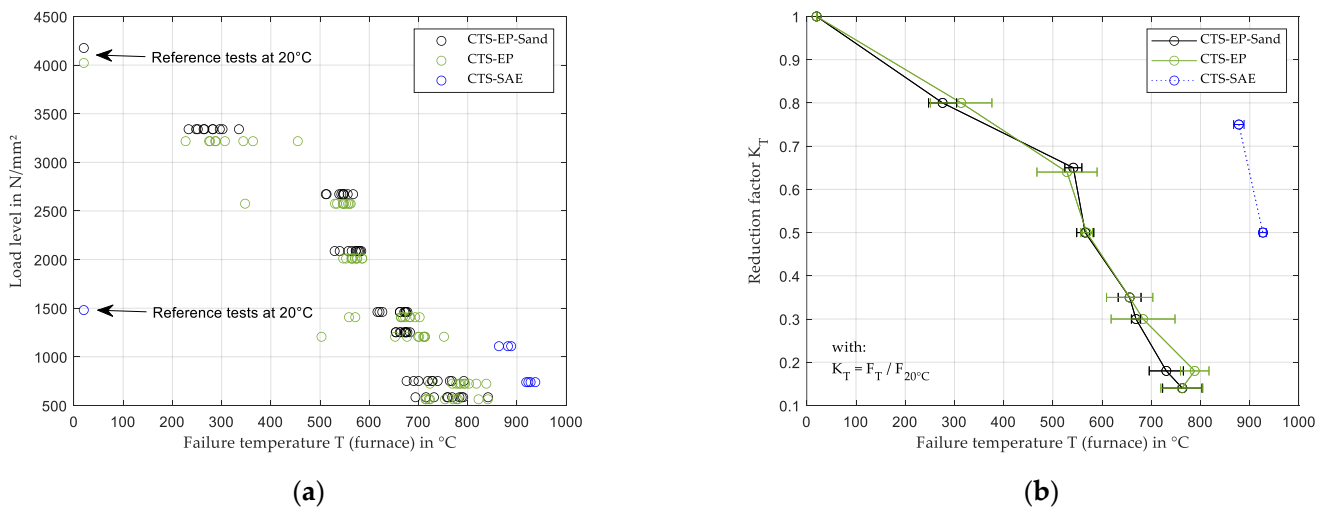


Figure 16. CTS transient test results. (a) Failure temperature measured in the furnace due to varying load levels (individual values); (b) Transient and stationary test temperatures as mean value with standard deviation for the reduction factor K_T .

To investigate the interface between the reinforcement and matrix different temperature-loaded CTS specimens were examined. For $K_T = 1.0/0.64/0.5/0.14$, a specimen was examined using scanning electron microscopy (SEM) images with backscattered electrons (BSE) at the Institute for Materials Applications in Mechanical Engineering, RWTH Aachen University. The SEM images of the reference specimens, also $K_T = 1.0$, show an intact impregnation or coating of the reinforcement and from fit bond to the mortar matrix, cf. Figure 17a,b. For $K_T < 0.64$, the rovings were pulled out of the CTS during the tests, and therefore only residues of weft direction rovings are visible on the SEM images. At $K_T = 0.64$, an impregnation layer of epoxy-resin was detected for the CTS-EP (Figure 17c), while only a few adherent polymer particles are still visible for the surface-modified reinforcement CTS-EP-Sand (Figure 17d). Moreover, the loose quartz sand and mortar matrix are depicted next to the weft roving in Figure 17d.

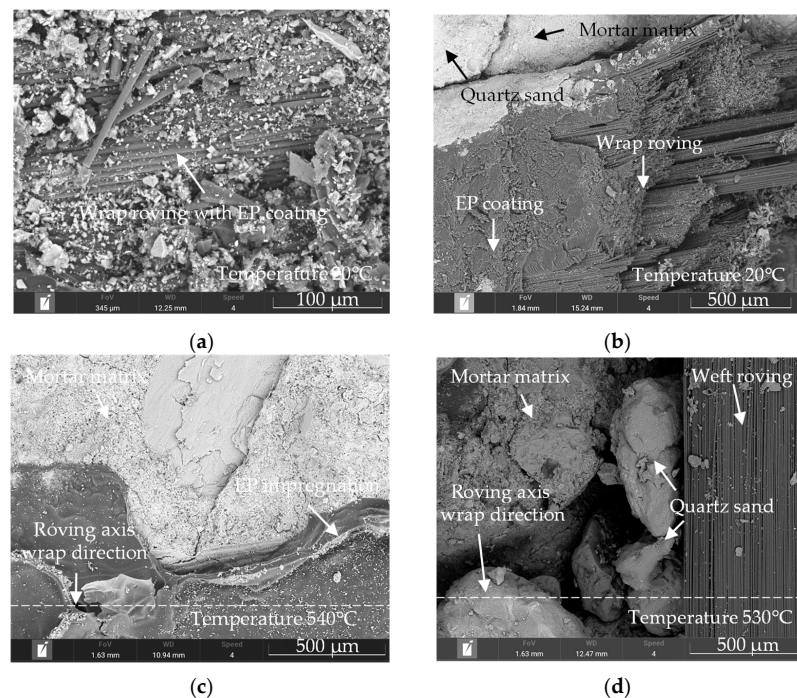


Figure 17. Cont.

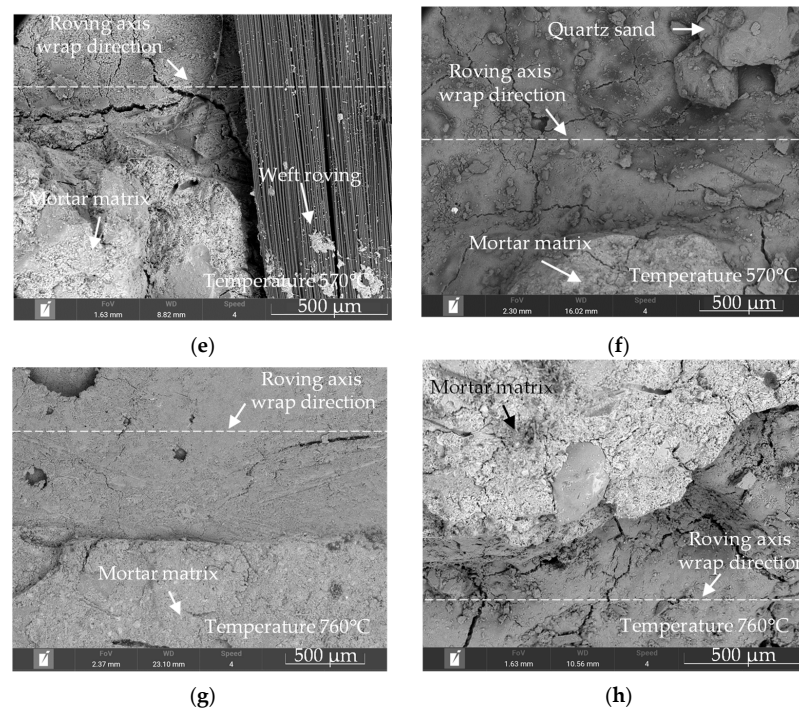


Figure 17. SEM images of CTS specimens after testing. (a) CTS-EP for $K_T = 1.0$; (b) CTS-EP-Sand for $K_T = 1.0$; (c) CTS-EP for $K_T = 0.64$; (d) CTS-EP-Sand for $K_T = 0.64$; (e) CTS-EP for $K_T = 0.5$; (f) CTS-EP-Sand for $K_T = 0.5$; (g) CTS-EP for $K_T = 0.14$; (h) CTS-EP-Sand for $K_T = 0.14$.

Moreover, for $K_T = 0.5$ no impregnation material is detectable any longer, even for CTS-EP, cf. Figure 17e. The impregnation on the weft roving was completely dissolved, and there was no longer any bond due to the gap between the reinforcement and the mortar. In Figure 17f, residues of the quartz sand and carbon filaments are detectable for the CTS-EP-Sand reinforcement. Furthermore, small cracks formed in the mortar matrix due to the elevated temperatures. In comparison, for $K_T = 0.14$, the cracks in the mortar on the specimen are wider for CTS-EP-Sand, cf. Figure 17h. In summary, the images show that for $K_T < 0.64$, the specimens have only a few polymeric adhesions and after the decomposition of the impregnation, no further bond between mortar and textile reinforcement exists.

According to Equation (2), the reduction factor was determined and interpolated in the temperature ranges for the investigated load levels of CTS, cf. Table 6. Due to the positive gradient of the interpolation and the high scatter for $K_T < 0.2$ for CTS-EP, the reduction factors are considered up to a temperature of 788 °C.

Table 6. Calculation table of temperature-dependent reduction factor of CTS for the reinforcement materials.

CTS-EP		CTS-EP-Sand		CTS-SAE	
Reduction Factors K_T (T)	Temperature Ranges T	Reduction Factors K_T (T)	Temperature Ranges T	Reduction Factors K_T (T)	Temperature Ranges T
[–]	[°C]	[–]	[°C]	[–]	[°C]
$-0.68 \cdot 10^{-3} \cdot T + 1.014$	$20 \leq T \leq 314$	$-0.78 \cdot 10^{-3} \cdot T + 1.016$	$20 \leq T \leq 276$	$-0.29 \cdot 10^{-3} \cdot T + 1.006$	$20 \leq T \leq 878$
$-0.67 \cdot 10^{-3} \cdot T + 1.009$	$314 \leq T \leq 539$	$-0.56 \cdot 10^{-3} \cdot T + 0.956$	$276 \leq T \leq 542$	$-5.10 \cdot 10^{-3} \cdot T + 5.229$	$878 \leq T \leq 927$
$-5.00 \cdot 10^{-3} \cdot T + 3.344$	$539 \leq T \leq 569$				
$-6.20 \cdot 10^{-3} \cdot T + 4.006$	$542 \leq T \leq 566$				
$-1.66 \cdot 10^{-3} \cdot T + 1.441$	$566 \leq T \leq 656$				
$-3.88 \cdot 10^{-3} \cdot T + 2.892$	$656 \leq T \leq 669$	$-1.95 \cdot 10^{-3} \cdot T + 1.603$	$669 \leq T \leq 730$		
		$-1.23 \cdot 10^{-3} \cdot T + 1.076$	$730 \leq T \leq 763$		

In Figure 18, the results of the rovings and CTS transient tensile strength tests are merged with the literature data. The experimentally obtained results are within the data

cloud of [1,6–10,15,19–21]. However, the scatter of the test results is considerable, so that a generalization of the reduction coefficients for all carbon textile reinforcements would lead to very conservative values [1]. For example, the results of the CTS are classified at the upper edge of the data cloud. As already described in Section 4.1.1, this is due to the high reference tensile strength. Compared to the epoxy-resin-impregnated CTRC by Holz [1], the reference strength has increased by 29% for the same carbon fiber and further developed impregnation. Furthermore, special attention should be paid to SAE, which shows very high temperatures compared to the results of other impregnations in terms of elevated temperature behavior.

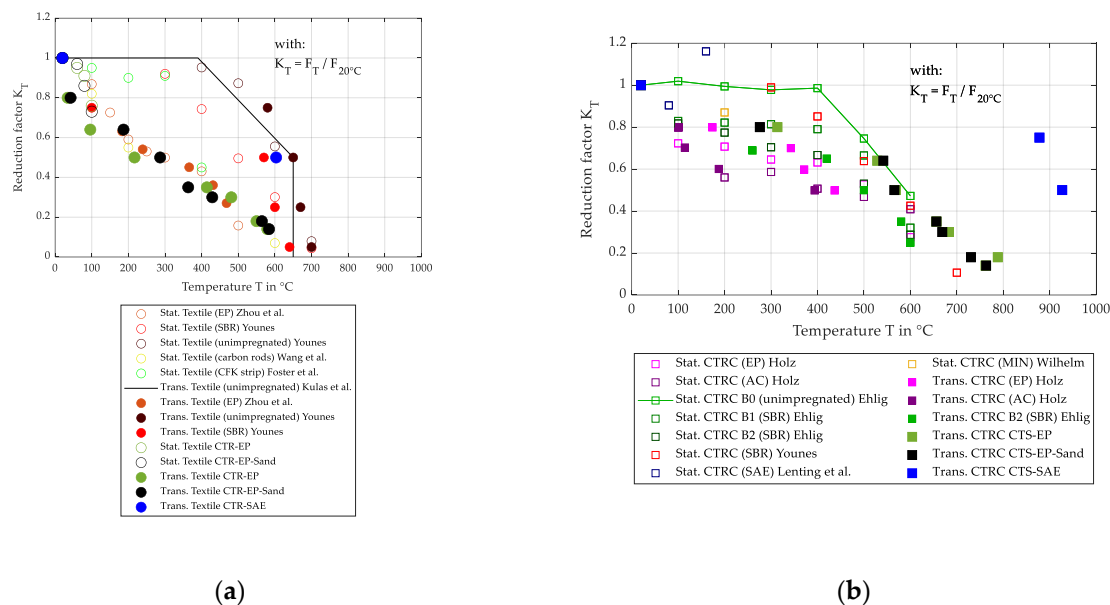


Figure 18. Results of the investigations on the elevated temperature behavior for the reduction factor K_T as a quotient of tensile strength at a specific temperature of 20 $^{\circ}\text{C}$, compared to examined results [1,6–10,15,19–21]. (a) Test results of the textile component; (b) Test results of the CTRC.

5. Conclusions and Outlook

Within the framework of this investigation, the elevated temperature behavior of carbon textile reinforcements for concrete structures up to 1000 $^{\circ}\text{C}$ was investigated. Based on the preliminary findings described, stationary and transient tests in a high-temperature furnace on the roving and CTS, as well as additional flame tests and thermogravimetrically analysis, were conducted. For this purpose, reinforcements with the inorganic impregnation material SAE, an epoxy-resin impregnation with and without additional quartz sand surface modification were investigated.

The key findings of this study can be summarized as follows:

- Overall, the failure temperature of the carbon textile reinforcement increases with decreasing tensile strength load levels. In addition to carbon fiber decomposition, impregnation decomposition also proved to be a decisive factor.
- For the roving component, the SAE impregnation resulted in higher failure temperatures in comparison to the epoxy-resin impregnation in comparable load levels. However, this significantly higher failure temperature must be considered together with the 64% lower absolute tensile strength at room temperature. For comparable tensile strengths, this can be neglected. Furthermore, the surface modification of epoxy-resin-impregnated textile reinforcement resulted in increasing failure temperatures up to 50% at tensile strength load levels above 50%, as the decomposition was slowed down by the increased resin content. Through the thermal analysis, the experimental results were comparatively evaluated, and a correlation between the experimental results and the decomposition process was obtained.

- Moreover, the flame tests evidenced flame and smoke development of both epoxy-resin-impregnated carbon textile reinforcements, whereas the SAE impregnation was not flammable. Compared to the CTR-EP, a 30% longer after-flaming time was measured for CTR-EP-Sand.
- Based on the results of the CTRC transient tensile strength tests, temperature-dependent reduction factors were derived for the material combinations with the 1 cm cover layer of the RM-A4 mortar. The results indicate a temperature shielding effect of the mortar layer up to 400 °C, which is most effective before the decomposition process occurs ($K_T > 0.64$).
- Compared to the literature findings, the results for epoxy-resin impregnated carbon textile reinforcement are in good agreement with the data cloud. However, the deviating reference strengths lead to different elevated temperature results for the same impregnation types. Comparing the impregnation materials, the SAE impregnation is classified at the upper edge of the data cloud close to the elevated temperature behavior of unimpregnated carbon fibers. The epoxy-resin impregnation material leads to greatest reduction for comparable temperature levels.

In future studies, further test series should be carried out on SAE impregnation and provide information on further tensile strength levels. The inorganic SAE reinforcement shows high performance potential at elevated temperatures. However, the impregnation process requires further improvement and the industrial production technology is yet to be developed.

Author Contributions: Conceptualization, methodology, software, validation, formal analysis, investigation, resources, data curation, writing—original draft preparation, visualization, A.D.; writing—review and editing, A.D., C.M.C. and M.R.; supervision, project administration, A.D. and C.M.C. All authors have read and agreed to the published version of the manuscript.

Funding: This research received no external funding.

Acknowledgments: The authors would like to thank Martin Lenting, FH Münster for the SAE reinforcement materials and Angelika Kiefel, Tobias Sedlatschek, as well as Malte Schmachtenberg, Institute for Materials Applications in Mechanical Engineering, RWTH Aachen, for the opportunity to use the SEM, and for the explanation as well as instruction. Furthermore, the authors would like to thank Univ.-Prof. Dr. rer. nat. Oliver Weichold, ibac, for the opportunity to use the burning chamber.

Conflicts of Interest: The authors declare no conflict of interest.

References

1. Holz, K. Carbon Reinforced Concrete Exposed to High Temperature. Ph.D. Thesis, Technische Universität Dresden, Dresden, Germany, 2021.
2. Morales Cruz, C. Crack-Distributing Carbon Textile Reinforced Concrete Protection Layers. Ph.D. Thesis, RWTH Aachen University, Aachen, Germany, 2020.
3. Jahami, A.; Tensah, Y.; Khatib, J.; Baalbaki, O.; Kenai, S. The behavior of CFRP strengthened RC beams subjected to blast loading. *Mag. Civ. Eng.* **2021**, *103*, 10309. [[CrossRef](#)]
4. Bielak, J. Shear in Slabs with Non-Metallic Reinforcement. Ph.D. Thesis, RWTH Aachen University, Aachen, Germany, 2021.
5. Mechtcherine, V.; Grafe, J.; Nerella, V.N.; Spaniol, E.; Hertel, M.; Füssel, U. 3D-printed steel reinforcement for digital concrete construction—Manufacture, mechanical properties and bond behaviour. *Constr. Build. Mater.* **2018**, *179*, 125–137. [[CrossRef](#)]
6. Kulas, C.; Hegger, J.; Raupach, M.; Antons, U. High-temperature behavior of textile reinforced concrete. In Proceedings of the International RILEM Conference on Advances in Construction Materials Through Science and Engineering, Hong Kong, China, 5–7 September 2011; pp. 827–834.
7. Wilhelm, K. Bond Behavior of Mineral- and Polymer-Bonded Carbon Reinforcement and Concrete at Room Temperature and Elevated Temperatures up to 500 °C. Ph.D. Thesis, Technische Universität Dresden, Dresden, Germany, 2021.
8. Younes, A. Experimental Analysis and Modeling of Mechanical Behavior of High Performance Fiber Materials under Long Term Load, High Temperature and Impact for Composites Applications. Ph.D. Thesis, Technische Universität Dresden, Dresden, Germany, 2013.
9. Ehlig, D. Load-Bearing Behaviour of Carbon Concrete as Bending Reinforcement of Reinforced Concrete Slabs under Fire Load. Ph.D. Thesis, Technische Universität Dresden, Dresden, Germany, 2018.

10. Lenting, M.; Orłowsky, J. Einaxiale Zugversuche an textilbewehrten Betonen mit anorganisch getränkten Carbonfasern. *Beton-Und Stahlbetonbau* **2020**, *115*, 495–503. [[CrossRef](#)]
11. *DIN EN 1992-1-2:2021-09*; Eurocode 2: Design of Concrete Structures—Part 1-2: General Rules—Structural Fire Design. German and English Version prEN 1992-1-2:2021. Beuth Verlag GmbH: Berlin, Germany, 2021.
12. *DIN EN 13501-1:2019-05*; Fire Classification of Construction Products and Building Elements—Part 1: Classification Using Data from Reaction to Fire Tests. German Version EN 13501-1:2018. Beuth Verlag GmbH: Berlin, Germany, 2019.
13. *DIN EN 13501-2:2016-12*; Fire Classification of Construction Products and Building Elements—Part 2: Classification Using Data from Fire Resistance Tests, Excluding Ventilation Services. German Version EN 13501-2:2016. Beuth Verlag GmbH: Berlin, Germany, 2016.
14. Nováková, I. Behavior of Cementitious Composites Exposed to High Temperatures. Ph.D. Thesis, Brno University of Technology, Brno, Czech Republic, 2020.
15. Kulas, C.; Hegger, J.; Raupach, M.; Antons, U. Experimental and theoretical investigations on the high-temperature behavior of fine-grained concrete and textile yarns. *Beton-Und Stahlbetonbau* **2011**, *106*, 707–715. [[CrossRef](#)]
16. Bisby, L.A. Fire Behaviour of Fibre-Reinforced Polymer (FRP) Reinforced or Confined Concrete. Ph.D. Thesis, Queen's University Kingston, Kingston, ON, Canada, 2003.
17. Bisby, L.A.; Williams, B.K.; Kodur, V.R.K.; Green, M.F.; Chowdhury, E. *Fire Performance of FRP Systems for Infrastructure: A State-of-the-Art Report*; Research Report 179; Queen's University, Kingston and National Research Council: Ottawa, ON, Canada, 2005. [[CrossRef](#)]
18. Bisby, L.A.; Green, M.F.; Kodur, V.K. Response to fire of concrete structures that incorporate FRP. *Prog. Struct. Eng. Mater.* **2005**, *7*, 136–149. [[CrossRef](#)]
19. Foster, S.K.; Bisby, L.A. High temperature residual properties of externally bonded FRP systems. In Proceedings of the 7th International Symposium on Fiber Reinforced Polymer Reinforcement for Reinforced Concrete Structures (FRPRCS-7) ACI SP230-70, Kansas City, MO, USA, 6–9 November 2005; pp. 1235–1252.
20. Wang, Y.C.; Kodur, V. Variation of strength and stiffness of fibre reinforced polymer reinforcing bars with temperature. *Cem. Concr. Compos.* **2005**, *27*, 864–874. [[CrossRef](#)]
21. Zhou, F.; Zhang, J.; Song, S.; Yang, D.; Wang, C. Effect of temperature on material properties of carbon fiber reinforced polymer (CFRP) tendons: Experiments and model assessment. *Materials* **2019**, *12*, 1025. [[CrossRef](#)] [[PubMed](#)]
22. Younes, A.; Seidel, A.; Engler, T.; Cherif, C. Materialverhalten von AR-Glas-und Carbonfilamentgarnen unter Dauerlast sowie unter Hochtemperatureinwirkung. In Proceedings of the 4th Colloquium on Textile Reinforced Structures (CTRS4), Dresden, Germany, 3–5 June 2009; pp. 1–16.
23. Ehlig, D.; Jesse, F.; Curbach, M. High temperature tests on textile reinforced concrete (TRC) strain specimens. In Proceedings of the 2nd International RILEM Conference on Material Science Textile Reinforced Concrete, Aachen, Germany, 6–8 September 2010; pp. 141–151.
24. Mechtcherine, V.; Schneider, K.; Brameshuber, W. 2—Mineral-based matrices for textile-reinforced concrete. In *Textile Fibre Composites in Civil Engineering*; Triantafyllou, T., Ed.; Woodhead Publishing: Soston, UK, 2016; pp. 25–43.
25. Technical Product Data Sheet—Solidian. Available online: <https://solidian.com/downloads/> (accessed on 27 October 2022).
26. *DIN EN ISO 11357-1:2017-02*; Plastics—Differential Scanning Calorimetry (DSC)—Part 1: General Principles (ISO 11357-1:2016). German Version EN ISO 11357-1:2016. Beuth Verlag GmbH: Berlin, Germany, 2017.
27. *DIN EN ISO 11357-2:2020-08*; Plastics—Differential Scanning Calorimetry (DSC)—Part 2: Determination of Glass Transition Temperature and Step Height (ISO 11357-2:2020). German Version EN ISO 11357-2:2020. Beuth Verlag GmbH: Berlin, Germany, 2020.
28. *DIN EN ISO 11358-1:2022-07*; Plastics—Thermogravimetry (TG) of Polymers—Part 1: General Principles (ISO 11358-1:2022). German Version EN ISO 11358-1:2022. Beuth Verlag GmbH: Berlin, Germany, 2022.
29. *TR IH*; Technische Regel—Instandhaltung von Betonbauwerken (TR Instandhaltung)—Teil 1: Anwendungsbereich und Planung der Instandhaltung. Deutsches Institut für Bautechnik (DIBt): Berlin, Germany, 2020.
30. *TR IH*; Technische Regel—Instandhaltung von Betonbauwerken (TR Instandhaltung)—Teil 2: Merkmale von Produkten oder Systemen für die Instand-Setzung und Regelungen für deren Verwendung. Deutsches Institut für Bautechnik (DIBt): Berlin, Germany, 2020.
31. Dahlhoff, A.; Winkels, B.; Morales Cruz, C.; Raupach, M. Investigations on the Experimental Setup for Testing the Centric Tensile Strength According to ASTM C307 of Mineral-based Materials. *J. Civ. Eng. Constr.* **2022**, *11*, 239–254. [[CrossRef](#)]
32. *DIN EN 60695-11-10 VDE 0471-11-10:2014-10*; Fire Hazard Testing—Part 11-10: Test Flames—50 W Horizontal and Vertical Flame Test Methods (IEC 60695-11-10:2013). German Version EN 60695-11-10:2013. Beuth Verlag GmbH: Berlin, Germany, 2014.
33. *DIN EN ISO 11925-2:2020-07*; Reaction to Fire Tests—Ignitability of Products Subjected to Direct Impingement of Flame—Part 2: Single-Flame Source Test (ISO 11925-2:2020). German Version EN ISO 11925-2:2020. Beuth Verlag GmbH: Berlin, Germany, 2020.
34. Hertzberg, T. Dangers relating to fires in carbon-fibre based composite material. *Fire Mater.* **2005**, *29*, 231–248. [[CrossRef](#)]
35. Greiner, L. Fiber Protection and Flame Retardancy of Carbon Fiber Reinforced Epoxy Resins. Ph.D. Thesis, Technische Universität Darmstadt, Darmstadt, Germany, 2020.
36. Razali, N.M.; Wah, Y.B. Power comparisons of shapiro-wilk, kolmogorov-smirnov, lilliefors and anderson-darling tests. *J. Stat. Modeling Anal.* **2011**, *2*, 21–33.
37. Grubbs, F.E. Procedures for detecting outlying observations in samples. *Technometrics* **1969**, *11*, 1–21. [[CrossRef](#)]